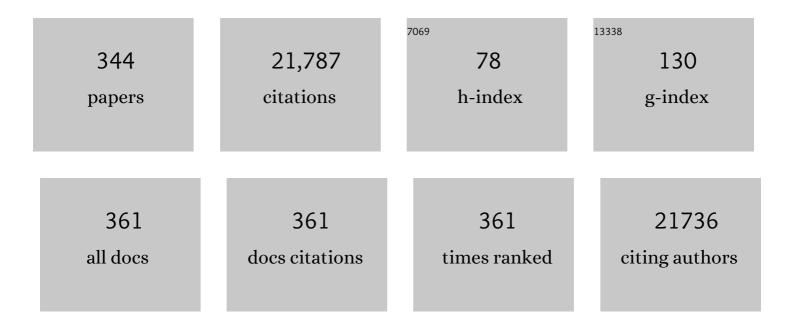
Jie-Sheng Chen

List of Publications by Year in descending order

Source: https://exaly.com/author-pdf/7771530/publications.pdf Version: 2024-02-01



#	Article	IF	CITATIONS
1	Photoluminescent Metalâ^'Organic Polymer Constructed from Trimetallic Clusters and Mixed Carboxylates. Inorganic Chemistry, 2003, 42, 944-946.	1.9	647
2	Metal-Free Activation of Dioxygen by Graphene/g-C ₃ N ₄ Nanocomposites: Functional Dyads for Selective Oxidation of Saturated Hydrocarbons. Journal of the American Chemical Society, 2011, 133, 8074-8077.	6.6	567
3	Janus Co/CoP Nanoparticles as Efficient Mott–Schottky Electrocatalysts for Overall Water Splitting in Wide pH Range. Advanced Energy Materials, 2017, 7, 1602355.	10.2	482
4	Surface and Interface Engineering of Electrode Materials for Lithiumâ€lon Batteries. Advanced Materials, 2015, 27, 527-545.	11.1	426
5	Structures, Photoluminescence, Up-Conversion, and Magnetism of 2D and 3D Rare-Earth Coordination Polymers with Multicarboxylate Linkages. Inorganic Chemistry, 2006, 45, 2857-2865.	1.9	403
6	Corrosion engineering towards efficient oxygen evolution electrodes with stable catalytic activity for over 6000 hours. Nature Communications, 2018, 9, 2609.	5.8	389
7	Extended Structures and Physicochemical Properties of Uranyl–Organic Compounds. Accounts of Chemical Research, 2011, 44, 531-540.	7.6	375
8	Activating Cobalt Nanoparticles via the Mott–Schottky Effect in Nitrogen-Rich Carbon Shells for Base-Free Aerobic Oxidation of Alcohols to Esters. Journal of the American Chemical Society, 2017, 139, 811-818.	6.6	351
9	Efficient oxygen evolution electrocatalysis in acid by a perovskite with face-sharing IrO6 octahedral dimers. Nature Communications, 2018, 9, 5236.	5.8	325
10	Synthesis, Structure, and Photoelectronic Effects of a Uraniumâ^'Zincâ^'Organic Coordination Polymer Containing Infinite Metal Oxide Sheets. Journal of the American Chemical Society, 2003, 125, 9266-9267.	6.6	302
11	Electrochemical Reduction of N ₂ into NH ₃ by Donor–Acceptor Couples of Ni and Au Nanoparticles with a 67.8% Faradaic Efficiency. Journal of the American Chemical Society, 2019, 141, 14976-14980.	6.6	290
12	Structural Variation from 1D to 3D: Effects of Ligands and Solvents on the Construction of Lead(II)–Organic Coordination Polymers. Chemistry - A European Journal, 2007, 13, 3248-3261.	1.7	280
13	Macroporous V ₂ O ₅ â^'BiVO ₄ Composites: Effect of Heterojunction on the Behavior of Photogenerated Charges. Journal of Physical Chemistry C, 2011, 115, 8064-8071.	1.5	251
14	Water-Insoluble Ag-U-Organic Assemblies with Photocatalytic Activity. Chemistry - A European Journal, 2005, 11, 2642-2650.	1.7	249
15	Surface Binding of Polypyrrole on Porous Silicon Hollow Nanospheres for Liâ€ l on Battery Anodes with High Structure Stability. Advanced Materials, 2014, 26, 6145-6150.	11.1	244
16	Carbon-Coated V ₂ O ₅ Nanocrystals as High Performance Cathode Material for Lithium Ion Batteries. Chemistry of Materials, 2011, 23, 5290-5292.	3.2	230
17	2D/2D Heterojunctions for Catalysis. Advanced Science, 2019, 6, 1801702.	5.6	224
18	New Polymerâ^'Inorganic Nanocomposites:Â PEOâ^'ZnO and PEOâ^'ZnOâ^'LiClO4Films. Journal of Physical Chemistry B, 2001, 105, 10169-10174.	1.2	221

#	Article	IF	CITATIONS
19	Hierarchical porous carbon derived from rice straw for lithium ion batteries with high-rate performance. Electrochemistry Communications, 2009, 11, 130-133.	2.3	218
20	A Novel Open-Framework Cobalt Phosphate Containing a Tetrahedrally Coordinated Cobalt(II) Center: CoPO4· 0.5 C2H10N2. Angewandte Chemie International Edition in English, 1994, 33, 639-640.	4.4	216
21	Preparation, Structures, and Photocatalytic Properties of Three New Uranylâ `Organic Assembly Compounds. Inorganic Chemistry, 2008, 47, 4844-4853.	1.9	210
22	Highly Efficient Dehydrogenation of Formic Acid over a Palladiumâ€Nanoparticleâ€Based Mott–Schottky Photocatalyst. Angewandte Chemie - International Edition, 2013, 52, 11822-11825.	7.2	210
23	Boosting selective nitrogen reduction to ammonia on electron-deficient copper nanoparticles. Nature Communications, 2019, 10, 4380.	5.8	203
24	A General Strategy for Fabricating Isolated Single Metal Atomic Site Catalysts in Y Zeolite. Journal of the American Chemical Society, 2019, 141, 9305-9311.	6.6	191
25	Montmorillonite-Supported Ag/TiO ₂ Nanoparticles: An Efficient Visible-Light Bacteria Photodegradation Material. ACS Applied Materials & Interfaces, 2010, 2, 544-550.	4.0	189
26	Efficient Sunlightâ€Driven Dehydrogenative Coupling of Methane to Ethane over a Zn ⁺ â€Modified Zeolite. Angewandte Chemie - International Edition, 2011, 50, 8299-8303.	7.2	187
27	MoO ₂ /Mo ₂ C Heteronanotubes Function as Highâ€Performance Liâ€lon Battery Electrode. Advanced Functional Materials, 2014, 24, 3399-3404.	7.8	185
28	One-pot synthesis of Ag–Fe3O4 nanocomposite: a magnetically recyclable and efficient catalyst for epoxidation of styrene. Chemical Communications, 2008, , 3414.	2.2	182
29	Vinylene-Bridged Two-Dimensional Covalent Organic Frameworks via Knoevenagel Condensation of Tricyanomesitylene. Journal of the American Chemical Society, 2020, 142, 11893-11900.	6.6	180
30	High stability and superior rate capability of three-dimensional hierarchical SnS2 microspheres as anode material in lithium ion batteries. Journal of Power Sources, 2011, 196, 3650-3654.	4.0	175
31	Encapsulating Palladium Nanoparticles Inside Mesoporous MFI Zeolite Nanocrystals for Shapeâ€Selective Catalysis. Angewandte Chemie - International Edition, 2016, 55, 9178-9182.	7.2	174
32	Three-Dimensional 3dâ^'4f Heterometallic Coordination Polymers:Â Synthesis, Structures, and Magnetic Properties. Inorganic Chemistry, 2005, 44, 5241-5246.	1.9	172
33	Strongly Veined Carbon Nanoleaves as a Highly Efficient Metalâ€Free Electrocatalyst. Angewandte Chemie - International Edition, 2014, 53, 6905-6909.	7.2	156
34	Highly Luminescent ZnO Nanocrystals Stabilized by Ionic-Liquid Components. Angewandte Chemie - International Edition, 2006, 45, 7370-7373.	7.2	153
35	Homochiral Porous Lanthanide Phosphonates with 1D Triple-Strand Helical Chains:  Synthesis, Photoluminescence, and Adsorption Properties. Inorganic Chemistry, 2006, 45, 4431-4439.	1.9	151
36	SAPO-18 Catalysts and Their Broensted Acid Sites. The Journal of Physical Chemistry, 1994, 98, 10216-10224.	2.9	149

#	Article	IF	CITATIONS
37	Direct conversion of urea into graphitic carbon nitride over mesoporous TiO ₂ spheres under mild condition. Chemical Communications, 2011, 47, 1066-1068.	2.2	148
38	Synthesis of Amphiphilic Superparamagnetic Ferrite/Block Copolymer Hollow Submicrospheres. Journal of the American Chemical Society, 2006, 128, 8382-8383.	6.6	141
39	Multifunctional Au–Co@CN Nanocatalyst for Highly Efficient Hydrolysis of Ammonia Borane. ACS Catalysis, 2015, 5, 388-392.	5.5	135
40	Construction of a microporous inorganic–organic hybrid compound with uranyl units. Chemical Communications, 2004, , 1814-1815.	2.2	134
41	Facile Synthesis of Thermal―and Photostable Titania with Paramagnetic Oxygen Vacancies for Visibleâ€Light Photocatalysis. Chemistry - A European Journal, 2013, 19, 2866-2873.	1.7	133
42	Distinguishing the Silanol Groups in the Mesoporous Molecular Sieve MCM-41. Angewandte Chemie International Edition in English, 1996, 34, 2694-2696.	4.4	132
43	Strategies to succeed in improving the lithium-ion storage properties of silicon nanomaterials. Journal of Materials Chemistry A, 2016, 4, 32-50.	5.2	130
44	Polyether-Grafted ZnO Nanoparticles with Tunable and Stable Photoluminescence at Room Temperature. Chemistry of Materials, 2005, 17, 3062-3064.	3.2	127
45	Schottky Barrier Induced Coupled Interface of Electron-Rich N-Doped Carbon and Electron-Deficient Cu: In-Built Lewis Acid–Base Pairs for Highly Efficient CO ₂ Fixation. Journal of the American Chemical Society, 2019, 141, 38-41.	6.6	123
46	Formation of hydronium at the Broensted site in SAPO-34 catalysts. The Journal of Physical Chemistry, 1993, 97, 8109-8112.	2.9	119
47	Toward Hydrogenâ€Free and Dendriteâ€Free Aqueous Zinc Batteries: Formation of Zincophilic Protective Layer on Zn Anodes. Advanced Science, 2022, 9, e2104866.	5.6	118
48	Effect of Heterojunction on the Behavior of Photogenerated Charges in Fe ₃ O ₄ @Fe ₂ O ₃ Nanoparticle Photocatalysts. Journal of Physical Chemistry C, 2011, 115, 8637-8642.	1.5	112
49	MAPO-18 (M ? Mg, Zn, Co): a new family of catalysts for the conversion of methanol to light olefins. Journal of the Chemical Society Chemical Communications, 1994, , 603.	2.0	105
50	Self-modification of titanium dioxide materials by Ti ³⁺ and/or oxygen vacancies: new insights into defect chemistry of metal oxides. RSC Advances, 2014, 4, 13979-13988.	1.7	101
51	Structure of an Unusual Aluminium Phosphate ([Al5P6O24H]2- 2[N(C2H5)3H]+ · 2H2O) JDF-20 with Large Elliptical Apertures. Journal of Solid State Chemistry, 1993, 102, 204-208.	1.4	100
52	Syntheses and photoluminescent properties of two uranyl-containing compounds with extended structures. Polyhedron, 2006, 25, 1359-1366.	1.0	100
53	Porous Titania with Heavily Self-Doped Ti ³⁺ for Specific Sensing of CO at Room Temperature. Inorganic Chemistry, 2013, 52, 5924-5930.	1.9	100
54	Highly Reversible Zinc Anode Enabled by a Cation-Exchange Coating with Zn-Ion Selective Channels. ACS Nano, 2022, 16, 6906-6915.	7.3	100

#	Article	lF	CITATIONS
55	Hydrothermal synthesis and photoluminescent properties of ZnWO4 and Eu3+-doped ZnWO4. Materials Letters, 2002, 55, 152-157.	1.3	98
56	3D-hierarchical SnS ₂ micro/nano-structures: controlled synthesis, formation mechanism and lithium ion storage performances. CrystEngComm, 2012, 14, 1364-1375.	1.3	98
57	On the Nature of the Active Site in a CoAPO-18 Solid Acid Catalyst. Angewandte Chemie International Edition in English, 1994, 33, 1871-1873.	4.4	96
58	Cobalt-Doped MnO ₂ Hierarchical Yolk–Shell Spheres with Improved Supercapacitive Performance. Journal of Physical Chemistry C, 2015, 119, 8465-8471.	1.5	96
59	A novel porous sheet aluminophosphate: Al3P4O16 3? 1.5[NH3(CH2)4NH3]2+. Journal of the Chemical Society Chemical Communications, 1992, , 929.	2.0	95
60	A Chiral Lead Borate Containing Infinite and Finite Chains Built up from BO4and BO3Units. Chemistry of Materials, 2002, 14, 1314-1318.	3.2	95
61	Anchoring Cobalt Nanocrystals through the Plane of Graphene: Highly Integrated Electrocatalyst for Oxygen Reduction Reaction. Chemistry of Materials, 2015, 27, 544-549.	3.2	95
62	Silicoaluminophosphate number eighteen (SAPO-18): a new microporous solid acid catalyst. Catalysis Letters, 1994, 28, 241-248.	1.4	92
63	Nitrogen-doped graphene microtubes with opened inner voids: Highly efficient metal-free electrocatalysts for alkaline hydrogen evolution reaction. Nano Research, 2016, 9, 2606-2615.	5.8	92
64	Tuning the Adsorption Energy of Methanol Molecules Along Niâ€Nâ€Doped Carbon Phase Boundaries by the Mott–Schottky Effect for Gasâ€Phase Methanol Dehydrogenation. Angewandte Chemie - International Edition, 2018, 57, 2697-2701.	7.2	91
65	Sol–gel preparation of efficient red phosphor Mg2TiO4:Mn4+ and XAFS investigation on the substitution of Mn4+ for Ti4+. Journal of Materials Chemistry C, 2013, 1, 4327.	2.7	90
66	A facile one-pot reduction method for the preparation of a SnO/SnO ₂ /GNS composite for high performance lithium ion batteries. Dalton Transactions, 2014, 43, 3137-3143.	1.6	89
67	Nitrogen-doped carbon nets with micro/mesoporous structures as electrodes for high-performance supercapacitors. Journal of Materials Chemistry A, 2016, 4, 16698-16705.	5.2	88
68	Oxygen Vacancy Engineering of Co ₃ O ₄ Nanocrystals through Coupling with Metal Support for Water Oxidation. ChemSusChem, 2017, 10, 2875-2879.	3.6	88
69	Synthesis of Ionic Vinyleneâ€Linked Covalent Organic Frameworks through Quaternizationâ€Activated Knoevenagel Condensation. Angewandte Chemie - International Edition, 2021, 60, 13614-13620.	7.2	87
70	Synergistic Effect on the Photoactivation of the Methane CH Bond over Ga ³⁺ â€Modified ETSâ€10. Angewandte Chemie - International Edition, 2012, 51, 4702-4706.	7.2	86
71	Strategies toward Highâ€Performance Cathode Materials for Lithium–Oxygen Batteries. Small, 2018, 14, e1800078.	5.2	86
72	Boosting the Zn-ion transfer kinetics to stabilize the Zn metal interface for high-performance rechargeable Zn-ion batteries. Journal of Materials Chemistry A, 2021, 9, 16814-16823.	5.2	86

#	Article	IF	CITATIONS
73	Bronsted, Lewis, and Redox Centers on CoAPO-18 Catalysts. 1. Vibrational Modes of Adsorbed Water. The Journal of Physical Chemistry, 1994, 98, 13350-13356.	2.9	85
74	MOFs of Uranium and the Actinides. Structure and Bonding, 2014, , 265-295.	1.0	84
75	Lithiation mechanism of hierarchical porous MoO ₂ nanotubes fabricated through one-step carbothermal reduction. Journal of Materials Chemistry A, 2014, 2, 80-86.	5.2	84
76	Synthesis, Structures and Electrochemical Properties of Nitro- and Amino-Functionalized Diiron Azadithiolates as Active Site Models of Fe-Only Hydrogenases. Chemistry - A European Journal, 2004, 10, 4474-4479.	1.7	83
77	A Composite of Carbonâ€Wrapped Mo ₂ C Nanoparticle and Carbon Nanotube Formed Directly on Ni Foam as a Highâ€Performance Binderâ€Free Cathode for Liâ€O ₂ Batteries. Advanced Functional Materials, 2016, 26, 8514-8520.	7.8	83
78	Hierarchical carbon nanopapers coupled with ultrathin MoS2 nanosheets: Highly efficient large-area electrodes for hydrogen evolution. Nano Energy, 2015, 15, 335-342.	8.2	81
79	Nonaqueous Synthesis and Characterization of a New 2-Dimensional Layered Aluminophosphate [Al3P4O16]3ⴴ· 3[CH3CH2NH3]+. Journal of Solid State Chemistry, 1997, 129, 37-44.	1.4	80
80	Multistaged discharge constructing heterostructure with enhanced solid-solution behavior for long-life lithium-oxygen batteries. Nature Communications, 2019, 10, 5810.	5.8	80
81	IR spectroscopic study of CD3CN adsorbed on ALPO-18 molecular sieve and the solid acid catalysts SAPO-18 and MeAPO-18. Journal of the Chemical Society, Faraday Transactions, 1994, 90, 3455.	1.7	79
82	Room-temperature transfer hydrogenation and fast separation of unsaturated compounds over heterogeneous catalysts in an aqueous solution of formic acid. Green Chemistry, 2014, 16, 3746-3751.	4.6	79
83	Neuron-Inspired Design of High-Performance Electrode Materials for Sodium-Ion Batteries. ACS Nano, 2018, 12, 11503-11510.	7.3	79
84	Preparation and gas storage of high surface area microporous carbon derived from biomass source cornstalks. Bioresource Technology, 2008, 99, 4803-4808.	4.8	76
85	Construction of Three-Dimensional Uranyl-Organic Frameworks with Benzenetricarboxylate Ligands. European Journal of Inorganic Chemistry, 2010, 2010, 3780-3788.	1.0	75
86	Solving the Structure of a Metal-Substituted Aluminum Phosphate Catalyst by Electron Microscopy, Computer Simulation, and X-ray Powder Diffraction. Angewandte Chemie International Edition in English, 1992, 31, 1472-1475.	4.4	74
87	A graphene-wrapped silver–porous silicon composite with enhanced electrochemical performance for lithium-ion batteries. Journal of Materials Chemistry A, 2013, 1, 13648.	5.2	74
88	Carbonate decomposition: Low-overpotential Li-CO2 battery based on interlayer-confined monodisperse catalyst. Energy Storage Materials, 2018, 15, 291-298.	9.5	73
89	Formation of Single-Crystalline CuS Nanoplates Vertically Standing on Flat Substrate. Crystal Growth and Design, 2007, 7, 2265-2267.	1.4	72
90	Controlled Synthesis, Growth Mechanism, and Properties of Monodisperse CdS Colloidal Spheres. Chemistry - A European Journal, 2007, 13, 8754-8761.	1.7	71

#	Article	IF	CITATIONS
91	An open-framework zinc phosphate with ZnOZn linkages. Advanced Materials, 1994, 6, 679-680.	11.1	70
92	Cobalt-substituted aluminophosphate molecular sieves: x-ray absorption, infrared spectroscopic, and catalytic studies. Chemistry of Materials, 1992, 4, 1373-1380.	3.2	69
93	Uranyl pyridine-dicarboxylate compounds with clustered water molecules. Inorganic Chemistry Communication, 2006, 9, 595-598.	1.8	68
94	Enriching Co nanoparticles inside carbon nanofibers via nanoscale assembly of metal–organic complexes for highly efficient hydrogen evolution. Nano Energy, 2016, 22, 79-86.	8.2	68
95	Schottky Barrierâ€Induced Surface Electric Field Boosts Universal Reduction of NO _{<i>x</i>} ^{â^'} in Water to Ammonia. Angewandte Chemie - International Edition, 2021, 60, 20711-20716.	7.2	68
96	Assembly of a manganese(ii) pyridine-3,4-dicarboxylate polymeric network based on infinite Mn–O–C chains. Dalton Transactions, 2003, , 28-30.	1.6	67
97	Synthesis of uranium oxide nanoparticles and their catalytic performance for benzyl alcohol conversion to benzaldehyde. Journal of Materials Chemistry, 2008, 18, 1146.	6.7	67
98	Towards real Li-air batteries: A binder-free cathode with high electrochemical performance in CO2 and O2. Energy Storage Materials, 2017, 7, 209-215.	9.5	66
99	Synthesis and structure of a new microporous anionic derivative of germanium dioxide: [Ge18O38(OH)4]8-[(C2N2H10)2+]4.cntdot.2H2O. Chemistry of Materials, 1992, 4, 808-812.	3.2	65
100	The First Organo-Templated Cobalt Phosphate with a Zeolite Topology. Inorganic Chemistry, 2000, 39, 1476-1479.	1.9	65
101	Free‣tanding Air Cathodes Based on 3D Hierarchically Porous Carbon Membranes: Kinetic Overpotential of Continuous Macropores in Liâ€O ₂ Batteries. Angewandte Chemie - International Edition, 2018, 57, 6825-6829.	7.2	65
102	Polarized few-layer g-C3N4 as metal-free electrocatalyst for highly efficient reduction of CO2. Nano Research, 2018, 11, 2450-2459.	5.8	65
103	Electrocatalyst design for aprotic Li–CO ₂ batteries. Energy and Environmental Science, 2020, 13, 4717-4737.	15.6	65
104	Lowâ€Overpotential Li–O ₂ Batteries Based on TFSI Intercalated Co–Ti Layered Double Oxides. Advanced Functional Materials, 2016, 26, 1365-1374.	7.8	64
105	Synthesis and structure of a novel large-pore microporous magnesium-containing aluminophosphate (DAF-1). Journal of the Chemical Society Chemical Communications, 1993, , 633.	2.0	63
106	Li ₄ Ti ₅ O ₁₂ /TiO ₂ Hollow Spheres Composed Nanoflakes with Preferentially Exposed Li ₄ Ti ₅ O ₁₂ (011) Facets for High-Rate Lithium Ion Batteries. ACS Applied Materials & Interfaces, 2014, 6, 19791-19796.	4.0	63
107	Heteroatomâ€Embedded Approach to Vinyleneâ€Linked Covalent Organic Frameworks with Isoelectronic Structures for Photoredox Catalysis. Angewandte Chemie - International Edition, 2022, 61, .	7.2	63
108	Uniform hierarchical MoO2/carbon spheres with high cycling performance for lithium ion batteries. Journal of Materials Chemistry A, 2013, 1, 12038.	5.2	62

#	Article	IF	CITATIONS
109	New chain architecture for a one-dimensional aluminophosphate, [H3NCH2CH2NH3][AlP2 O8H]. Chemical Communications, 1997, , 1273-1274.	2.2	61
110	Chemical Formation of Mononuclear Univalent Zinc in a Microporous Crystalline Silicoaluminophosphate. Journal of the American Chemical Society, 2003, 125, 6622-6623.	6.6	61
111	Synthesis and Characterization of a Family of Amine-Intercatalated Lamellar Aluminophosphates from Alcoholic System. Chemistry of Materials, 1997, 9, 457-462.	3.2	60
112	Fabrication and Growth Mechanism of Selenium and Tellurium Nanobelts through a Vacuum Vapor Deposition Route. Journal of Physical Chemistry C, 2007, 111, 12926-12932.	1.5	60
113	Carbon nanocages with nanographene shell for high-rate lithium ion batteries. Journal of Materials Chemistry, 2010, 20, 9748.	6.7	60
114	Nitrogen-doped carbon nanotube sponge with embedded Fe/Fe ₃ C nanoparticles as binder-free cathodes for high capacity lithium–sulfur batteries. Journal of Materials Chemistry A, 2018, 6, 17473-17480.	5.2	60
115	Interfacial Approach toward Benzeneâ€Bridged Polypyrrole Film–Based Microâ€Supercapacitors with Ultrahigh Volumetric Power Density. Advanced Functional Materials, 2020, 30, 1908243.	7.8	60
116	Organo-template control of inorganic structures: a low-symmetry two-dimensional sheet aluminophosphate3[NH3CHMeCH2NH3][Al6P8O32]·H2O. Chemical Communications, 1996, , 1781-1782.	2.2	59
117	In situ catalytic growth of large-area multilayered graphene/MoS2 heterostructures. Scientific Reports, 2014, 4, 4673.	1.6	58
118	Synthesis and Structure of a Chain Aluminophosphate Filled with [NH4]+and [H3NCH2CH2NH3]2+Cations. Journal of Solid State Chemistry, 1996, 127, 145-150.	1.4	57
119	Constructing holey graphene monoliths via supramolecular assembly: Enriching nitrogen heteroatoms up to the theoretical limit for hydrogen evolution reaction. Nano Energy, 2015, 15, 567-575.	8.2	57
120	Controlled Growth and Photocatalytic Properties of CdS Nanocrystals Implanted in Layered Metal Hydroxide Matrixes. Journal of Physical Chemistry B, 2005, 109, 21602-21607.	1.2	56
121	Synthesis, structure characterization and photocatalytic properties of two new uranyl naphthalene-dicarboxylate coordination polymer compounds. Inorganic Chemistry Communication, 2010, 13, 1542-1547.	1.8	55
122	Syntheses, Structures, and Magnetic Properties of Mixed-Valent Diruthenium(II,III) Diphosphonates with Discrete and One-Dimensional Structures. Inorganic Chemistry, 2005, 44, 4309-4314.	1.9	54
123	Atomic‣cale Mott–Schottky Heterojunctions of Boron Nitride Monolayer and Graphene as Metalâ€Free Photocatalysts for Artificial Photosynthesis. Advanced Science, 2018, 5, 1800062.	5.6	54
124	Enhanced Electrochemical Performance of Aprotic Li O ₂ Batteries with a Ruthenium omplexâ€Based Mobile Catalyst. Angewandte Chemie - International Edition, 2021, 60, 16404-16408.	7.2	53
125	A Green Chemistry of Graphene: Photochemical Reduction towards Monolayer Graphene Sheets and the Role of Water Adlayers. ChemSusChem, 2012, 5, 642-646.	3.6	52
126	Nonâ€Conjugated Dicarboxylate Anode Materials for Electrochemical Cells. Angewandte Chemie - International Edition, 2018, 57, 8865-8870.	7.2	52

#	Article	IF	CITATIONS
127	Heterojunctionâ€Based Electron Donators to Stabilize and Activate Ultrafine Pt Nanoparticles for Efficient Hydrogen Atom Dissociation and Gas Evolution. Angewandte Chemie - International Edition, 2021, 60, 25766-25770.	7.2	52
128	Synthesis and characterization of Cd–Cr and Zn–Cd–Cr layered double hydroxides intercalated with dodecyl sulfate. Journal of Solid State Chemistry, 2005, 178, 1830-1836.	1.4	50
129	Formation of CuS nanotube arrays from CuCl Nanorods through a gas-solid reaction route. Journal of Crystal Growth, 2007, 299, 386-392.	0.7	50
130	Microporous carbon derived from pinecone hull as anode material for lithium secondary batteries. Materials Letters, 2007, 61, 5209-5212.	1.3	50
131	Heterometal Alkoxides as Precursors for the Preparation of Porous Fe– and Mn–TiO ₂ Photocatalysts with High Efficiencies. Chemistry - A European Journal, 2008, 14, 11123-11131.	1.7	50
132	Mesoporous titania rods as an anode material for high performance lithium-ion batteries. Journal of Power Sources, 2012, 214, 298-302.	4.0	50
133	Template-directed metal oxides for electrochemical energy storage. Energy Storage Materials, 2016, 3, 1-17.	9.5	50
134	Photoluminescent and photovoltaic properties observed in a zinc borate Zn2(OH)BO3. Journal of Materials Chemistry, 2003, 13, 2227-2233.	6.7	49
135	A uranium–zinc–organic molecular compound containing planar tetranuclear uranyl units. Dalton Transactions, 2003, , 4219-4220.	1.6	49
136	Controlled modification of multiwalled carbon nanotubes with Zno nanostructures. Journal of Solid State Chemistry, 2008, 181, 822-827.	1.4	49
137	Hierarchical Li4Ti5O12/TiO2 composite tubes with regular structural imperfection for lithium ion storage. Scientific Reports, 2013, 3, 3490.	1.6	49
138	A precursor route to single-crystalline WO3 nanoplates with an uneven surface and enhanced sensing properties. Dalton Transactions, 2012, 41, 9773.	1.6	48
139	Light-induced formation of porous TiO2 with superior electron-storing capacity. Chemical Communications, 2010, 46, 2112.	2.2	46
140	Towards ultra-stable lithium metal batteries: Interfacial ionic flux regulated through LiAl LDH-modified polypropylene separator. Chemical Engineering Journal, 2020, 395, 125187.	6.6	46
141	Preparation and Tunable Photoluminescence of Carbogenic Nanoparticles Confined in a Microporous Magnesium-Aluminophosphate. Inorganic Chemistry, 2010, 49, 5859-5867.	1.9	45
142	Wrinkled Graphene Monoliths as Superabsorbing Building Blocks for Superhydrophobic and Superhydrophilic Surfaces. Angewandte Chemie - International Edition, 2015, 54, 15165-15169.	7.2	45
143	Toward Lower Overpotential through Improved Electron Transport Property: Hierarchically Porous CoN Nanorods Prepared by Nitridation for Lithium–Oxygen Batteries. Nano Letters, 2016, 16, 5902-5908.	4.5	43
144	Grouping Effect of Single Nickelâ^'N ₄ Sites in Nitrogenâ€Ðoped Carbon Boosts Hydrogen Transfer Coupling of Alcohols and Amines. Angewandte Chemie - International Edition, 2018, 57, 15194-15198.	7.2	43

#	Article	IF	CITATIONS
145	Structure and magnetic properties of a novel copper diphosphonate with pillared layered structure:. Journal of Solid State Chemistry, 2004, 177, 1297-1301.	1.4	42
146	Magnetically recyclable Ag-ferrite catalysts: general synthesis and support effects in the epoxidation of styrene. Dalton Transactions, 2009, , 10527.	1.6	42
147	Photochemically Engineering the Metal–Semiconductor Interface for Roomâ€Temperature Transfer Hydrogenation of Nitroarenes with Formic Acid. Chemistry - A European Journal, 2014, 20, 16732-16737.	1.7	42
148	Controlled modification of multi-walled carbon nanotubes with CuO, Cu2O and Cu nanoparticles. Solid State Sciences, 2009, 11, 655-659.	1.5	40
149	Incorporation of heterostructured Sn/SnO nanoparticles in crumpled nitrogen-doped graphene nanosheets for application as anodes in lithium-ion batteries. Chemical Communications, 2014, 50, 9961-9964.	2.2	40
150	Synthetic porous materials applied in hydrogenation reactions. Microporous and Mesoporous Materials, 2017, 237, 246-259.	2.2	40
151	Dual Function of Racemic Isopropanolamine as Solvent and as Template for the Synthesis of a New Layered Aluminophosphate: [NH3CH2CH(OH)CH3]3·Al3P4O16. Journal of Solid State Chemistry, 2000, 151, 145-149.	1.4	39
152	Unambiguous Observation of Electron Transfer from a Zeolite Framework to Organic Molecules. Angewandte Chemie - International Edition, 2009, 48, 6678-6682.	7.2	39
153	Constructing Ohmic contact in cobalt selenide/Ti dyadic electrode: The third aspect to promote the oxygen evolution reaction. Nano Energy, 2017, 39, 321-327.	8.2	39
154	Mixed-bonded open-framework aluminophosphates and related layered materials. Topics in Catalysis, 1999, 9, 93-103.	1.3	38
155	Graphene-nanosheet-wrapped LiV3O8 nanocomposites as high performance cathode materials for rechargeable lithium-ion batteries. Journal of Power Sources, 2016, 307, 426-434.	4.0	38
156	The synthesis and crystal structure of a novel clay-like gallophosphate with sub-unit-cell intergrowths of ethylenediamine: [GaPO4(OH)]–0·5(H3NCH2CH2NH3)2+. Journal of the Chemical Society Chemical Communications, 1991, , 1520-1522.	2.0	37
157	A Metal-Rich Fluorinated Indium Phosphate, 4[NH3(CH2)3NH3]·3[H3O]·[In9(PO4)6(HPO4)2F16]·3H2O, with 14-Membered Ring Channels. Chemistry of Materials, 1998, 10, 773-776.	3.2	37
158	Effects of raw material texture and activation manner on surface area of porous carbons derived from biomass resources. Journal of Colloid and Interface Science, 2008, 327, 108-114.	5.0	37
159	Room-temperature spontaneous crystallization of porous amorphous titania into a high-surface-area anatase photocatalyst. Chemical Communications, 2013, 49, 8217.	2.2	37
160	New Families of M(III)X(V)O4-Type Microporous Crystals and Inclusion Compounds. Studies in Surface Science and Catalysis, 1991, 60, 63-72.	1.5	36
161	Absorption spectra of Se and HgI2 chains in channels of AlPO4-5 single crystal. Applied Physics Letters, 1997, 70, 34-36.	1.5	36
162	Hierarchical porous carbon spheres as an anode material for lithium ion batteries. RSC Advances, 2013, 3, 10823.	1.7	36

#	Article	IF	CITATIONS
163	A Polyimide Nanolayer as a Metalâ€Free and Durable Organic Electrode Toward Highly Efficient Oxygen Evolution. Angewandte Chemie - International Edition, 2018, 57, 12563-12566.	7.2	36
164	Germanium nanoparticles supported by 3D ordered macroporous nickel frameworks as high-performance free-standing anodes for Li-ion batteries. Chemical Engineering Journal, 2018, 354, 616-622.	6.6	36
165	Co ₃ O ₄ -based binder-free cathodes for lithium–oxygen batteries with improved cycling stability. Dalton Transactions, 2015, 44, 8678-8684.	1.6	35
166	Activating Oxygen Molecules over Carbonylâ€Modified Graphitic Carbon Nitride: Merging Supramolecular Oxidation with Photocatalysis in a Metalâ€Free Catalyst for Oxidative Coupling of Amines into Imines. ChemCatChem, 2016, 8, 3441-3445.	1.8	35
167	Free-standing hybrid porous membranes integrated with transition metal nitride and carbide nanoparticles for high-performance lithium-sulfur batteries. Chemical Engineering Journal, 2019, 378, 122208.	6.6	35
168	Converting waste paper to multifunctional graphene-decorated carbon paper: from trash to treasure. Journal of Materials Chemistry A, 2015, 3, 13926-13932.	5.2	34
169	Well-ordered mesoporous Fe ₂ O ₃ /C composites as high performance anode materials for sodium-ion batteries. Dalton Transactions, 2017, 46, 5025-5032.	1.6	34
170	Hydroquinone Resin Induced Carbon Nanotubes on Ni Foam As Binder-Free Cathode for Li–O ₂ Batteries. ACS Applied Materials & Interfaces, 2016, 8, 3868-3873.	4.0	33
171	Two Porous Polyoxometalate-Resorcin[4]arene-Based Supramolecular Complexes: Selective Adsorption of Organic Dyes and Electrochemical Properties. Crystal Growth and Design, 2018, 18, 6046-6053.	1.4	33
172	Surface modification of Ni foam for stable and dendrite-free lithium deposition. Chemical Engineering Journal, 2021, 405, 127022.	6.6	32
173	Synthesis and X-ray crystal structures of two new alkaline-earth metal borates: SrBO2(OH) and Ba3B6O9(OH)6. Dalton Transactions RSC, 2002, , 2031-2035.	2.3	31
174	Synthesis and Structural Characterization of a New Layered Aluminophosphate Intercalated with Triply-Protonated Triethylenetetramine [C6H21N4][Al3P4O16]. Journal of Solid State Chemistry, 1999, 146, 458-463.	1.4	30
175	Hydrothermal synthesis and photoluminesent properties of Sb3+-doped and (Sb3+,Mn2+)-co-doped calcium hydroxyapatite. Journal of Materials Chemistry, 2002, 12, 3761-3765.	6.7	30
176	Polyether-grafted SnO2 nanoparticles designed for solid polymer electrolytes with long-term stabilityElectronic supplementary information (ESI) available: XPS results and in situ IR spectra. See http://www.rsc.org/suppdata/jm/b4/b405179c/. Journal of Materials Chemistry, 2004, 14, 2775.	6.7	30
177	Nanoscale Kirkendall growth of silicalite-1 zeolite mesocrystals with controlled mesoporosity and size. Chemical Communications, 2015, 51, 12563-12566.	2.2	30
178	Ultra-durable two-electrode Zn–air secondary batteries based on bifunctional titania nanocatalysts: a Co ²⁺ dopant boosts the electrochemical activity. Journal of Materials Chemistry A, 2016, 4, 7841-7847.	5.2	30
179	Mild and selective hydrogenation of CO2 into formic acid over electron-rich MoC nanocatalysts. Science Bulletin, 2020, 65, 651-657.	4.3	30
180	Preparation and structural characterization of a novel galloarsenate using a dimethylamine template. Journal of the Chemical Society Chemical Communications, 1989, , 1217.	2.0	29

#	Article	IF	CITATIONS
181	Ein neues Cobaltphosphat mit Hohlraumstruktur und tetraedrisch koordinierten Co ^{II} â€Zentren: CoPO ₄ · 0.5 C ₂ H ₁₀ N ₂ . Angewandte Chemie, 1994, 106, 667-668.	1.6	29
182	Synthesis and characterization of a novel layered titanium silicate JDF-L1. Journal of Materials Chemistry, 1996, 6, 1827.	6.7	29
183	Synthesis and structural characterisation of two- and three-dimensional fluorinated indium phosphates. Chemical Communications, 1997, , 781-782.	2.2	29
184	Amorphous silicon with high specific surface area prepared by a sodiothermic reduction method for supercapacitors. Chemical Communications, 2013, 49, 5007.	2.2	29
185	The crystallinity effect of mesocrystalline BaZrO ₃ hollow nanospheres on charge separation for photocatalysis. Chemical Communications, 2014, 50, 3021-3023.	2.2	29
186	Synthesis and structure of a novel aluminoarsenate with an open framework. Journal of the Chemical Society Chemical Communications, 1989, , 810.	2.0	28
187	Infrared Study on the Dehydroxylation of C60-Loaded MCM-41. Langmuir, 1997, 13, 2050-2054.	1.6	28
188	Hydrothermal Synthesis and Characterization of Two New Three-Dimensional Titanium Phosphates. Chemistry of Materials, 2001, 13, 2017-2022.	3.2	28
189	Controlled synthesis of magnetic Pd/Fe3O4 spheres via an ethylenediamine-assisted route. Dalton Transactions, 2012, 41, 3204.	1.6	28
190	Porous vanadium-doped titania with active hydrogen: a renewable reductant for chemoselective hydrogenation of nitroarenes under ambient conditions. Chemical Communications, 2012, 48, 9032.	2.2	28
191	Boosting Potassium Storage Capacity Based on Stressâ€Induced Sizeâ€Dependent Solidâ€Solution Behavior. Advanced Energy Materials, 2018, 8, 1802175.	10.2	28
192	Surface engineering donor and acceptor sites with enhanced charge transport for low-overpotential lithium–oxygen batteries. Energy Storage Materials, 2020, 25, 52-61.	9.5	28
193	Boosting the electrochemical performance of Li–O2 batteries with DPPH redox mediator and graphene-luteolin-protected lithium anode. Energy Storage Materials, 2020, 31, 373-381.	9.5	28
194	Synthesis of SAPO-41 and SAPO-44 and their performance as acidic catalysts in the conversion of methanol to hydrocarbons. Catalysis Letters, 1991, 11, 199-207.	1.4	27
195	On the crystallisation and nature of the microporous boron–aluminium oxo chloride BAC(10). Journal of Materials Chemistry, 1996, 6, 465-468.	6.7	27
196	Enhanced oxygen electroreduction over nitrogen-free carbon nanotube-supported CuFeO ₂ nanoparticles. Journal of Materials Chemistry A, 2018, 6, 4331-4336.	5.2	27
197	Isoelectric Si Heteroatoms as Electron Traps for N ₂ Fixation and Activation. Advanced Functional Materials, 2020, 30, 2005779.	7.8	26
198	Controlled growth of Sb2O5nanoparticles and their use as polymer electrolyte fillers. Journal of Materials Chemistry, 2003, 13, 1994-1998.	6.7	25

#	Article	IF	CITATIONS
199	Synthesis of SnO2 hollow nanostructures with controlled interior structures through a template-assisted hydrothermal route. Dalton Transactions, 2011, 40, 8517.	1.6	25
200	Thiophene Derivative as a High Electrochemical Active Anode Material for Sodium-Ion Batteries: The Effect of Backbone Sulfur. Chemistry of Materials, 2018, 30, 8426-8430.	3.2	25
201	Real-space imaging of molecular sieves composed of aluminum phosphates and their metal-substituted analogs. The Journal of Physical Chemistry, 1992, 96, 8206-8209.	2.9	24
202	Effect of Surface Cations on Photoelectric Conversion Property of Nanosized Zirconia. Journal of Physical Chemistry C, 2009, 113, 9114-9120.	1.5	24
203	Cerium vanadate nanoparticles as a new anode material for lithium ion batteries. RSC Advances, 2013, 3, 7403.	1.7	24
204	Activating Pd nanoparticles on sol–gel prepared porous g-C ₃ N ₄ /SiO ₂ via enlarging the Schottky barrier for efficient dehydrogenation of formic acid. Inorganic Chemistry Frontiers, 2016, 3, 1124-1129.	3.0	24
205	Freeâ€Standing Air Cathodes Based on 3D Hierarchically Porous Carbon Membranes: Kinetic Overpotential of Continuous Macropores in Liâ€O ₂ Batteries. Angewandte Chemie, 2018, 130, 6941-6945.	1.6	24
206	Mesoporous H-ZSM-5 nanocrystals with programmable number of acid sites as "solid ligands―to activate Pd nanoparticles for C–C coupling reactions. Nano Research, 2018, 11, 874-881.	5.8	24
207	Engineering the Interfaces of Superadsorbing Grapheneâ€Based Electrodes with Gas and Electrolyte to Boost Gas Evolution and Activation Reactions. ChemSusChem, 2018, 11, 2306-2309.	3.6	24
208	Free-standing N,Co-codoped TiO ₂ nanoparticles for LiO ₂ -based Li–O ₂ batteries. Journal of Materials Chemistry A, 2019, 7, 23046-23054.	5.2	24
209	Electrochemical activation of C–H by electron-deficient W2C nanocrystals for simultaneous alkoxylation and hydrogen evolution. Nature Communications, 2021, 12, 3882.	5.8	24
210	Sol–gel synthesis and magnetization study of Mn1â^'xCuxFe2O4 (x=0, 0.2) nanocrystallites. Solid State Communications, 2004, 131, 519-522.	0.9	23
211	Decomposition of CO2 to carbon and oxygen under mild conditions over a zinc-modified zeolite. Chemical Communications, 2012, 48, 2325.	2.2	23
212	Programmable synthesis of mesoporous ZSM-5 nanocrystals as selective and stable catalysts for the methanol-to-propylene process. Catalysis Science and Technology, 2016, 6, 5262-5266.	2.1	23
213	Synergy of Fe-N4 and non-coordinated boron atoms for highly selective oxidation of amine into nitrile. Nano Research, 2020, 13, 2079-2084.	5.8	23
214	Sodium phthalate as an anode material for sodium ion batteries: effect of the bridging carbonyl group. Journal of Materials Chemistry A, 2020, 8, 8469-8475.	5.2	23
215	Preparation of hollow layered MoO3 microspheres through a resin template approach. Journal of Solid State Chemistry, 2005, 178, 390-394.	1.4	22
216	Phenoxymethylpenicillin-intercalated hydrotalcite as a bacteria inhibitor. Journal of Chemical Technology and Biotechnology, 2006, 81, 89-93.	1.6	22

#	Article	IF	CITATIONS
217	Decoration of multiwalled carbon nanotubes with CoO and NiO nanoparticles and studies of their magnetism properties. Journal of Colloid and Interface Science, 2009, 337, 272-277.	5.0	22
218	Dandelion-clock-inspired preparation of core-shell TiO2@MoS2 composites for high performance sodium ion storage. Journal of Alloys and Compounds, 2020, 815, 152386.	2.8	22
219	Zur Unterscheidung der Silanolgruppen im mesoporösen Molekularsieb MCMâ€41. Angewandte Chemie, 1995, 107, 2898-2900.	1.6	21
220	Core–shell anatase anode materials for sodium-ion batteries: the impact of oxygen vacancies and nitrogen-doped carbon coating. Nanoscale, 2019, 11, 17860-17868.	2.8	21
221	MoS2 nanoflakes integrated in a 3D carbon framework for high-performance sodium-ion batteries. Journal of Alloys and Compounds, 2019, 797, 1126-1132.	2.8	21
222	3D ordered macroporous MoO ₂ attached on carbonized cloth for high performance free-standing binder-free lithium–sulfur electrodes. Journal of Materials Chemistry A, 2019, 7, 24524-24531.	5.2	21
223	Dendrite-free lithium anode achieved under lean-electrolyte condition through the modification of separators with F-functionalized Ti3C2 nanosheets. Journal of Energy Chemistry, 2022, 66, 366-373.	7.1	21
224	Boosting Mass Exchange between Pd/NC and MoC/NC Dual Junctions via Electron Exchange for Cascade CO ₂ Fixation. Journal of the American Chemical Society, 2022, 144, 5418-5423.	6.6	21
225	The effect of Al3+ treatment on charge dynamics in dye-sensitized nanocrystalline TiO2 solar cells explored by photovoltage measurements. Materials Chemistry and Physics, 2010, 122, 259-261.	2.0	20
226	Photocatalytic Stille Cross-coupling on Gold/g-C3N4 Nano-heterojunction. Chemical Research in Chinese Universities, 2020, 36, 1013-1016.	1.3	20
227	Chemical fixation of CO ₂ on nanocarbons and hybrids. Journal of Materials Chemistry A, 2021, 9, 20857-20873.	5.2	20
228	Hydrothermal synthesis and luminescent properties of Sb3+-doped Sr3(PO4)2. Journal of Solid State Chemistry, 2004, 177, 3114-3118.	1.4	19
229	Syntheses, structures and properties of three cluster-based coordination polymers: influence of the metal ions on the ligand coordination mode and crystal chirality. Inorganica Chimica Acta, 2004, 357, 1389-1396.	1.2	19
230	Investigation into the role of MgO in the synthesis of MAPO-11 large single crystals. Microporous and Mesoporous Materials, 2005, 79, 79-84.	2.2	19
231	Spontaneous superlattice formation of ZnO nanocrystals capped with ionic liquid molecules. Chemical Communications, 2007, , 4131.	2.2	19
232	Light-Driven Preparation, Microstructure, and Visible-Light Photocatalytic Property of Porous Carbon-Doped TiO ₂ . International Journal of Photoenergy, 2012, 2012, 1-9.	1.4	19
233	Accelerated room-temperature crystallization of ultrahigh-surface-area porous anatase titania by storing photogenerated electrons. Chemical Communications, 2017, 53, 1619-1621.	2.2	19
234	The solution-phase process of a g-C ₃ N ₄ /BiVO ₄ dyad to a large-area photoanode: interfacial synergy for highly efficient water oxidation. Chemical Communications, 2017, 53, 10544-10547.	2.2	19

#	Article	IF	CITATIONS
235	Tuning the Adsorption Energy of Methanol Molecules Along Niâ€Nâ€Doped Carbon Phase Boundaries by the Mott–Schottky Effect for Gasâ€Phase Methanol Dehydrogenation. Angewandte Chemie, 2018, 130, 2727-2731.	1.6	19
236	Oriented arrays of Co3O4 nanoneedles for highly efficient electrocatalytic water oxidation. Chemical Communications, 2019, 55, 3971-3974.	2.2	19
237	General Synthesis of Uniform Metal Sulfide Colloidal Particles via Autocatalytic Surface Growth: A Self-Correcting System. Inorganic Chemistry, 2009, 48, 3132-3138.	1.9	18
238	Bio-inspired noble metal-free reduction of nitroarenes using NiS _{2+x} /g-C ₃ N ₄ . RSC Advances, 2014, 4, 60873-60877.	1.7	18
239	Crystal Structure of the Ergothioneine Sulfoxide Synthase from <i>Candidatus Chloracidobacterium thermophilum</i> and Structure-Guided Engineering To Modulate Its Substrate Selectivity. ACS Catalysis, 2019, 9, 6955-6961.	5.5	18
240	Formation of single-crystal cobalt-substituted gallophosphate LTA from an alcoholic system. Microporous Materials, 1996, 5, 333-336.	1.6	17
241	Light-Driven Transformation of ZnS-Cyclohexylamine Nanocomposite into Zinc Hydroxysulfate: A Photochemical Route to Inorganic Nanosheets. Inorganic Chemistry, 2011, 50, 9106-9113.	1.9	17
242	Synthesis and Structural Characterization of a New Open-Framework Tin(II) Phosphate:Â [Sn4(PO4)3]-·0.5[C4N2H12]2+. Inorganic Chemistry, 2000, 39, 1820-1822.	1.9	16
243	Single-site photocatalysts with a porous structure. Proceedings of the Royal Society A: Mathematical, Physical and Engineering Sciences, 2012, 468, 2099-2112.	1.0	16
244	Hydrothermal synthesis and characterization of a new boron-aluminium oxochloride. Polyhedron, 1996, 15, 4127-4132.	1.0	15
245	Synthesis and structural characterisation of a new layered aluminophosphate [C3H12N2][Al2P2O8(OH)2]·H2O. Dalton Transactions RSC, 2000, , 1981-1984.	2.3	15
246	Preparation and characterization of magadiite grafted with an azobenzene derivative. Solid State Sciences, 2004, 6, 1001-1006.	1.5	15
247	Sensor material based on occluded trisulfur anionic radicals for convenient detection of trace amounts of water molecules. Journal of Materials Chemistry, 2010, 20, 3307.	6.7	15
248	Single-Step Replacement of an Unreactive C–H Bond by a C–S Bond Using Polysulfide as the Direct Sulfur Source in the Anaerobic Ergothioneine Biosynthesis. ACS Catalysis, 2020, 10, 8981-8994.	5.5	15
249	{M(C5H4N)CH(OH)PO3}(H2O)Â(M = Mn, Fe, Co): layered compounds based on [hydroxy(4-pyridyl)methyl]phosphonate. Dalton Transactions, 2003, , 953-956.	1.6	14
250	Synergistic effect of BrÃ,nsted acid and platinum on purification of automobile exhaust gases. Scientific Reports, 2013, 3, 2349.	1.6	14
251	Monoâ€Atomic Fe Centers in Nitrogen/Carbon Monolayers for Liquidâ€Phase Selective Oxidation Reaction. ChemCatChem, 2018, 10, 3539-3545.	1.8	14
252	Synthesis of Ionic Vinylene‣inked Covalent Organic Frameworks through Quaternizationâ€Activated Knoevenagel Condensation. Angewandte Chemie, 2021, 133, 13726-13732.	1.6	14

#	Article	IF	CITATIONS
253	Facilitating Hot Electron Injection from Graphene to Semiconductor by Rectifying Contact for Vis–NIRâ€Driven H ₂ O ₂ Production. Small, 2022, 18, e2200885.	5.2	14
254	Bimodal mesopore distribution in a silica prepared by calcining a wet surfactant-containing silicate gel. Journal of the Chemical Society Chemical Communications, 1995, , 2367.	2.0	13
255	Synthesis and characterization of an unusual lamellar aluminophosphate synthesized from an alcohol system. Journal of the Chemical Society Dalton Transactions, 1996, , 3303.	1.1	13
256	Synthesis, structures and photoluminescence of two Er(III) coordination polymers. Journal of Coordination Chemistry, 2008, 61, 945-955.	0.8	13
257	Chemical "top-down―synthesis of amphiphilic superparamagnetic Fe ₃ O ₄ nanobelts from exfoliated FeOCI layers. Dalton Transactions, 2014, 43, 16173-16177.	1.6	13
258	In situ growth of ultrafine tin oxide nanocrystals embedded in graphitized carbon nanosheets for use in high-performance lithium-ion batteries. Journal of Materials Chemistry A, 2014, 2, 6960-6965.	5.2	13
259	Uric Acid as an Electrochemically Active Compound for Sodium-Ion Batteries: Stepwise Na ⁺ -Storage Mechanisms of Ĩ€-Conjugation and Stabilized Carbon Anion. ACS Applied Materials & Interfaces, 2017, 9, 33934-33940.	4.0	13
260	Atomically Dispersed Ni-Based Anti-Coking Catalysts for Methanol Dehydrogenation in a Fixed-Bed Reactor. ACS Catalysis, 2020, 10, 12569-12574.	5.5	13
261	The Synthesis and Characterization of a Two-Dimensional Cobaltâ^'Zinc Phosphate:Â NH4[Zn2-xCox(PO4)(HPO4)] (xâ‰^ 0.12)§. Journal of Physical Chemistry B, 1997, 101, 9940-9942.	1.2	12
262	12-Tungstosilicic acid doped polyethylene oxide as a proton conducting polymer electrolyte. Materials Chemistry and Physics, 2003, 80, 537-540.	2.0	12
263	Cu2SnSe3/CNTs Composite as a Promising Anode Material for Sodium-ion Batteries. Chemical Research in Chinese Universities, 2020, 36, 91-96.	1.3	12
264	Schottky Barrierâ€Induced Surface Electric Field Boosts Universal Reduction of NO x â^' in Water to Ammonia. Angewandte Chemie, 2021, 133, 20879-20884.	1.6	12
265	Towards High-performance Lithium-Sulfur Batteries: the Modification of Polypropylene Separator by 3D Porous Carbon Structure Embedded with Fe3C/Fe Nanoparticles. Chemical Research in Chinese Universities, 2022, 38, 147-154.	1.3	12
266	Synthesis and characterization of aluminophosphate molecular sieve AlPO4-41 from alcohol systems. Microporous Materials, 1996, 7, 219-223.	1.6	11
267	A Two-coordinate Copper(I) Complex Constructed from Cyanuric Acid and 4,4′-Bipyridyl: Synthesis, Structure and Photoluminescence. Chinese Journal of Chemistry, 2006, 24, 1045-1049.	2.6	11
268	A Facile Route to Mesoporous Carbon Catalyst Support Modified with Magnetic Nanoparticles. Chemistry Letters, 2007, 36, 422-423.	0.7	11
269	New indium selenite-oxalate and indium oxalate with two- and three-dimensional structures. Journal of Solid State Chemistry, 2009, 182, 102-106.	1.4	11
270	Rubber-based carbon electrode materials derived from dumped tires for efficient sodium-ion storage. Dalton Transactions, 2018, 47, 4885-4892.	1.6	11

#	Article	IF	CITATIONS
271	Autoxidation of polythiophene tethered to carbon cloth boosts its electrocatalytic activity towards durable water oxidation. Journal of Materials Chemistry A, 2020, 8, 19793-19798.	5.2	11
272	Synthesis of various indium phosphates in the presence of amine templates. Studies in Surface Science and Catalysis, 1997, 105, 397-404.	1.5	10
273	A three-dimensional framework constructed from gadolinium(III) and molybdenum through linkage of pyridine-2,5-dicarboxylate groups. Journal of Molecular Structure, 2007, 827, 114-120.	1.8	10
274	Synthesis, structure and photoluminescence of two zinc carboxylate polymers with different coordination architectures. Chinese Journal of Chemistry, 2003, 21, 1305-1308.	2.6	10
275	Elucidation of the chemical environment for zinc species in an electron-rich zinc-incorporated zeolite. Journal of Solid State Chemistry, 2013, 202, 111-115.	1.4	10
276	Transitions from a Kondo-like diamagnetic insulator into a modulated ferromagnetic metal in FeGa _{3â^'y} Ge _y . Proceedings of the National Academy of Sciences of the United States of America, 2018, 115, 3273-3278.	3.3	10
277	Nitrogen-thermal modification of the bifunctional interfaces of transition metal/carbon dyads for the reversible hydrogenation and dehydrogenation of heteroarenes. Chemical Communications, 2019, 55, 11394-11397.	2.2	10
278	Phosphazene-derived stable and robust artificial SEI for protecting lithium anodes of Li–O ₂ batteries. Chemical Communications, 2020, 56, 12566-12569.	2.2	10
279	Thiophene derivatives as electrode materials for high-performance sodium-ion batteries. Journal of Materials Chemistry A, 2021, 9, 11530-11536.	5.2	10
280	Heteroatomâ€Embedded Approach to Vinyleneâ€Linked Covalent Organic Frameworks with Isoelectronic Structures for Photoredox Catalysis. Angewandte Chemie, 2022, 134, e202111627.	1.6	10
281	In situ hydrothermal preparation of CdS/polymer composite particles with cadmium-containing polymer latexes. Materials Letters, 2004, 58, 384-386.	1.3	9
282	Carbon nanocolumn arrays prepared by pulsed laser deposition for lithium ion batteries. Journal of Power Sources, 2012, 203, 140-144.	4.0	9
283	A Polyimide Nanolayer as a Metalâ€Free and Durable Organic Electrode Toward Highly Efficient Oxygen Evolution. Angewandte Chemie, 2018, 130, 12743-12746.	1.6	9
284	Photogenerated singlet oxygen over zeolite-confined carbon dots for shape selective catalysis. Science China Chemistry, 2019, 62, 434-439.	4.2	9
285	Biomimetic Design of a 3 D Transition Metal/Carbon Dyad for the One‣tep Hydrodeoxygenation of Vanillin. ChemSusChem, 2020, 13, 1900-1905.	3.6	9
286	A novel 3D network coordination polymer consisting of paddlewheel Co 3 clusters connected by PO 4 and 4-pyridinecarboxylate. Inorganic Chemistry Communication, 2003, 6, 1429-1432.	1.8	8
287	Distinct effect of hierarchical structure on performance of anatase as an anode material for lithium-ion batteries. RSC Advances, 2013, 3, 26052.	1.7	8
288	Trapping oxygen in hierarchically porous carbon nano-nets: graphitic nitrogen dopants boost the electrocatalytic activity. RSC Advances, 2016, 6, 56765-56771.	1.7	8

#	Article	IF	CITATIONS
289	Mesoporous <scp>TS</scp> â€l Nanocrystals as Low Cost and High Performance Catalysts for Epoxidation of Styrene. Chinese Journal of Chemistry, 2017, 35, 577-580.	2.6	8
290	Designed electron-deficient gold nanoparticles for a room-temperature Csp3–Csp3 coupling reaction. Chemical Communications, 2021, 57, 741-744.	2.2	8
291	Oxygen Vacancy Engineering of Titania-Induced by Sr2+ Dopants for Visible-Light-Driven Hydrogen Evolution. Inorganic Chemistry, 2021, 60, 32-36.	1.9	8
292	Regulating Phase Junction and Oxygen Vacancies of TiO2 Nanoarrays for Boosted Photoelectrochemical Water Oxidation. Chemical Research in Chinese Universities, 2022, 38, 1292-1300.	1.3	8
293	Mesolamellar molybdenum sulfides with intercalated cetyltrimethylammonium cations. Inorganic Chemistry Communication, 2000, 3, 129-131.	1.8	7
294	Eu3+and Lysine Co-intercalated Â-Zirconium Phosphate and Its Catalytic Activity for Copolymerization of Propylene Oxide and CO2. Catalysis Letters, 2004, 94, 95-102.	1.4	7
295	Grouping Effect of Single Nickelâ^'N 4 Sites in Nitrogenâ€Doped Carbon Boosts Hydrogen Transfer Coupling of Alcohols and Amines. Angewandte Chemie, 2018, 130, 15414-15418.	1.6	7
296	Electrostatically mediated selectivity of Pd nanocatalyst via rectifying contact with semiconductor: Replace ligands with light. Applied Catalysis B: Environmental, 2018, 238, 404-409.	10.8	7
297	Synergy of B and Al Dopants in Mesoporous MFI Nanocrystals for Highly Selective Alcoholysis of Furfuryl Alcohol into Ethyl Levulinate. Energy Technology, 2019, 7, 1900271.	1.8	7
298	Heterojunctionâ€Based Electron Donators to Stabilize and Activate Ultrafine Pt Nanoparticles for Efficient Hydrogen Atom Dissociation and Gas Evolution. Angewandte Chemie, 2021, 133, 25970-25974.	1.6	7
299	Construction of Large Non‣ocalized Ï€â€Electron System for Enhanced Sodiumâ€ŀon Storage. Small, 2022, 18, e2105825.	5.2	7
300	Design of Functional Carbon Composite Materials for Energy Conversion and Storage. Chemical Research in Chinese Universities, 2022, 38, 677-687.	1.3	7
301	Supramolecular nano-assemblies with tailorable surfaces: recyclable hard templates for engineering hollow nanocatalysts. Science China Materials, 2014, 57, 7-12.	3.5	6
302	Preparation of Porous Silicon by Sodiothermic Reduction of Zeolite and Photoactivation for Benzene Oxidation. European Journal of Inorganic Chemistry, 2015, 2015, 1330-1333.	1.0	6
303	Direct reduction of oxygen gas over dendritic carbons with hierarchical porosity: beyond the diffusion limitation. Inorganic Chemistry Frontiers, 2018, 5, 2023-2030.	3.0	6
304	Towards high performance lithium-oxygen batteries: Co3O4-NiO heterostructure induced preferential growth of ultrathin Li2O2 film. Journal of Alloys and Compounds, 2021, 863, 158073.	2.8	6
305	Experimental Validation of the Importance of Thermally Stable Bulk Reduction States in TiO ₂ for Gas Sensor Applications. Acta Chimica Sinica, 2012, 70, 1477.	0.5	6
306	Synthesis and characterization of two aluminoarsenates with occluded ethylenediamine. Journal of the Chemical Society Dalton Transactions, 1990, , 3319.	1.1	5

#	Article	IF	CITATIONS
307	Host–guest Functional Materials. , 2011, , 405-428.		5
308	Use of Nitrogen-Containing Carbon Supports To Control the Acidity of Supported Heteropolyacid Model Catalysts. Industrial & Engineering Chemistry Research, 2018, 57, 13999-14010.	1.8	5
309	Mild hydrothermal preparation of a layered metal hydroxide salt with microtube/rod morphology. Particuology, 2010, 8, 192-197.	2.0	4
310	Synthesis and Characterization of Ethylenediammonium Molybdenum Thiocomplex [H ₃ NCH ₂ CH ₂ NH ₃][Mo ₃ S ₁₃]. Chinese Journal of Chemistry, 2001, 19, 681-688.	2.6	4
311	Formation of a built-in field at the porphyrin/ITO interface directly proven by the time-resolved photovoltage technique. Physical Chemistry Chemical Physics, 2015, 17, 5202-5206.	1.3	4
312	Top-down fabrication of hierarchical nanocubes on nanosheets composite for high-rate lithium storage. Dalton Transactions, 2018, 47, 16155-16163.	1.6	4
313	A New Route to Cyclohexanone using H ₂ CO ₃ as a Molecular Catalytic Ligand to Boost the Thorough Hydrogenation of Nitroarenes over Pd Nanocatalysts. ChemCatChem, 2019, 11, 2837-2842.	1.8	4
314	Enhanced Electrochemical Performance of Aprotic Liâ€CO ₂ Batteries with a Ruthenium omplexâ€Based Mobile Catalyst. Angewandte Chemie, 2021, 133, 16540-16544.	1.6	4
315	Rapidly and mildly transferring anatase phase of graphene-activated TiO2 to rutile with elevated Schottky barrier: Facilitating interfacial hot electron injection for Vis-NIR driven photocatalysis. Nano Research, 2022, 15, 10142-10147.	5.8	4
316	Towards high-performance lithium metal batteries: sol electrolyte generated with mesoporous silica. Chemical Engineering Journal, 2022, 446, 137421.	6.6	4
317	Synthesis and Characterization of a New Layered Barium Aluminate Containing Six-Membered Rings: BaAl2O3(OH)2·H2O. Journal of Solid State Chemistry, 2001, 161, 243-248.	1.4	3
318	Solvothermal Synthesis and Characterization of Zn(NH ₃)CO ₃ Single Crystal. Materials Research Society Symposia Proceedings, 2004, 817, 130.	0.1	3
319	Roomâ€Temperature Activation of Molecular Oxygen Over a Metalâ€Free Triazineâ€Decorated sp ² â€Carbon Framework for Green Synthesis. ChemCatChem, 2018, 10, 5331-5335.	1.8	3
320	Carbon monoliths with programmable valence bands as de novo anodes for additive-free coupling of alcohols into acetals. FlatChem, 2021, 27, 100248.	2.8	3
321	Structural Chemistry of Microporous Materials. , 0, , 19-116.		2
322	Carbon anode material formed from template molecules occluded in a magnesium-substituted aluminophosphate. Materials Chemistry and Physics, 2009, 113, 309-313.	2.0	2
323	(Ć ₁₄ N ₁₄ H ₆₃)´Na (H ₂ Mo ₆ P ₄ O ₃₁) ₂ · 8H ₂ O and (C ₁₄ N ₁₄ H ₆₃) Na (H ₂ Mo ₆ P ₄ O ₃₁) ₂ · 5H ₂ O.	2.6	2
324	Chinese Journal of Chemistry, 2002, 20, 858-864. Self-Oriented Single Crystalline Silicon Nanorod Arrays through a Chemical Vapor Reaction Route. Journal of Physical Chemistry C, 2010, 114, 2471-2475.	1.5	2

#	Article	IF	CITATIONS
325	Impact of photogenerated charge behaviors on luminescence of Eu3+-incorporated microporous titanosilicate ETS-10. Science China Chemistry, 2013, 56, 428-434.	4.2	2
326	Grand Challenges for Colloidal Materials and Interfaces: Dancing on Nano-Stage. Frontiers in Materials, 2014, 1, .	1.2	2
327	New routes for synthesizing mesoporous material. Studies in Surface Science and Catalysis, 1997, , 77-84.	1.5	1
328	A family of unusual lamellar aluminophosphates synthesized from non-aqueous systems. Studies in Surface Science and Catalysis, 1997, , 389-396.	1.5	1
329	Synthesis and characterization of novel open-framework cobalt phosphates from aqueous-alcoholic systems. Studies in Surface Science and Catalysis, 1997, 105, 381-388.	1.5	1
330	Preparation and characterization of semiconductor-organic films with a mesolamellar structure. Materials Letters, 2002, 52, 24-28.	1.3	1
331	Microporous carbon from biomass. Studies in Surface Science and Catalysis, 2007, , 1479-1485.	1.5	1
332	Facile preparation and cellular imaging of photoluminescent carbogenic nanoparticles derived from defoliations. Chemical Research in Chinese Universities, 2013, 29, 189-192.	1.3	1
333	Semiconductorâ€based nanocomposites for selective organic synthesis. Nano Select, 2021, 2, 1799.	1.9	1
334	Tunable Surface Electric Field of Electrocatalysts via Constructing Schottky Heterojunctions for Selective Conversion of Trash Ions to Treasures. Chemistry - A European Journal, 2022, 28, .	1.7	1
335	Chemical Formation of Mononuclear Univalent Zinc in a Microporous Crystalline Silicoaluminophosphate ChemInform, 2003, 34, no.	0.1	Ο
336	Hydrothermal Synthesis of Ce3+ and Tb3+ co-doped Ca3Al2(OH)12 Luminescent Material. Materials Research Society Symposia Proceedings, 2004, 817, 136.	0.1	0
337	Synthesis, Structures and Electrochemical Properties of Nitro- and Amino-Functionalized Diiron Azadithiolates as Active Site Models of Fe-Only Hydrogenases. Chemistry - A European Journal, 2005, 11, 803-803.	1.7	0
338	Synthetic Chemistry of Microporous Compounds (II)- Special Compositions, Structures, and Morphologies. , 0, , 191-266.		0
339	Towards Rational Design and Synthesis of Inorganic Microporous Materials. , 0, , 397-466.		0
340	Porous Host-Guest Advanced Materials. , 0, , 603-666.		0
341	Chapter 5. Structural Diversity and Potential Applications of Metal–Organic Coordination Polymers. , 2007, , 76-94.		0
342	Formation of nanographite using GaPO ₄ ‣TA as template. Chinese Journal of Chemistry, 2004, 22, 1399-1402.	2.6	0

#	Article	IF	CITATIONS
343	Materials Research at Shanghai Jiao Tong University. Advanced Materials, 2015, 27, 400-402.	11.1	0
344	SYNTHESIS AND X-RAY CRYSTAL STRUCTURES OF LOW-DIMENSIONAL BORATES FROM HYDROTHERMAL AND SOLVOTHERMAL SYSTEMS. , 2002, , .		0